

## Electron and positron scattering from the benzene derivative: Toluene

H. Kato,<sup>1</sup> C. Makochekanwa,<sup>1,2,\*</sup> Y. Shiroyama,<sup>2</sup> M. Hoshino,<sup>1</sup> N. Shinohara,<sup>3</sup> O. Sueoka,<sup>4</sup> M. Kimura,<sup>2</sup> and H. Tanaka<sup>1</sup>

<sup>1</sup>*Department of Physics, Sophia University, Tokyo 102-8554, Japan*

<sup>2</sup>*Graduate School of Sciences, Kyushu University, Fukuoka 812-8581, Japan*

<sup>3</sup>*Graduate School of Medicine, Yamaguchi University, Yamaguchi 755-8505, Japan*

<sup>4</sup>*Faculty of Engineering, Yamaguchi University, Yamaguchi 755-8611, Japan*

(Received 13 February 2007; published 14 June 2007)

Electron and positron cross sections for scattering from toluene molecules have been investigated both experimentally and theoretically over the energy range 0.4–1000 eV. Peaks have been observed in the electron total cross sections (TCSs) at 1.4, 4.5, and 8.0 and a shoulder at about 40 eV. Vibrational and elastic differential cross section experiments were carried out to probe the origin and nature of these peaks. The continuum multiple scattering method was used to calculate elastic integral cross sections for electron impact. Although the 1.4 eV peak is dominated by the elastic channel, strong contributions from the CH<sub>3</sub> asymmetric bending and stretching vibrational modes are also observed. The 4.5 eV feature is also observed to be strongly due to vibrational excitation. The broad 7–13 eV peak includes contributions from the CH<sub>3</sub> asymmetric bending (peaked at 7 eV) and the CH<sub>3</sub> stretching (peaked at 9.5 eV) vibrational modes. Positron TCSs are studied and compared to positron-benzene TCSs. The effect of the CH<sub>3</sub> substitution is observed to make a significant contribution to both electron and positron TCSs below 20 eV.

DOI: [10.1103/PhysRevA.75.062705](https://doi.org/10.1103/PhysRevA.75.062705)

PACS number(s): 34.80.Bm, 34.80.Dp, 36.10.Dr

### I. INTRODUCTION

For more than half of the last century benzene and mono-substituted benzene-derived organic compounds have invited some research interest owing to their usefulness in various industrial applications, albeit compromised by potential environmental problems arising from their toxicity. These molecules are also essential as basic training grounds for quantum-chemical calculations, including the Hückel method, because of their  $\pi$  electrons. The founding theoretical works on benzene observed that in excitation cross sections the  $\pi$  electrons are clearly easy to promote to the lowest excited levels [1,2].

The substitution of any H atom(s) from the benzene molecular structure results in either donation or extraction of electron(s) to or from the ring with a significant effect on the physical and chemical properties of the resulting molecules, for example, electron affinities [3], thermal electron mobilities [4], rate constants for electron attachment [5], and basicities [6]. Some interesting phenomena that have been observed so far to be characteristic of these benzene-derived molecules include (i) the lifting of the degeneracy of the two lowest unoccupied  $\pi$  orbitals, (ii) shifts in the positions of the peaks corresponding to compound-negative-ion states observed in threshold-electron-excitation (TEE) spectra [7], and (iii) enhancement of scattering cross sections due to the additional contribution from electron attachment (see [8,9] and references therein). In general, electron capture by these molecules involves  $\pi^*$  molecular orbitals and thus serves as a probe of the effect of the substitution of an H atom by an atom or radical upon  $\pi^*$  orbital energies.

A significant amount of theoretical and experimental work exists for electron scattering from benzene (C<sub>6</sub>H<sub>6</sub>). Theoretical work includes, (e.g., [1,2]), while experimental studies ranging from threshold electron excitation (TEE) [7], electron transmission experiments [10], vibrational and triplet excitation [12], and total cross section measurements [11,13,14] have been reported. To our knowledge, the only available studies in toluene (C<sub>6</sub>H<sub>5</sub>CH<sub>3</sub>) relevant to this work include the use of mechanical models to establish its model vibrational and Raman frequencies [15], infrared absorption coefficient spectra [16], argon collision-induced intramolecular energy flow studies in highly excited toluene [17], and some computer assisted structure verification and interpretation of the infrared and Raman spectra [18]. We are not aware of any reports in literature describing theoretical or experimental differential cross sections (DCSs), vibrational excitation, or total cross sections (TCSs) involving electron and positron interaction with toluene molecules. The only electron impact study directly related to the current work is the electron transmission study of resonant scattering of 0.5–11 eV electrons which reported resonances in toluene [19].

It was observed in these previous studies that the substitution of an atom or radical lowers the symmetry of the benzene ring and that the degenerate  $e_{2u}$  orbital of the benzene molecule is split into two in the energy range 0–2 eV [20]. Nevertheless electron transmission and other spectra of the benzene derivatives are seen to be largely uniform and to resemble that of the benzene molecule, despite the large changes in symmetry. In all three of the previous studies on toluene [3,15,19], the substitution of an H atom in benzene by CH<sub>3</sub>, a radical that donates electrons to the benzene ring, results in (i) a shift to lower Raman frequencies of the observed peaks in benzene spectra [3], (ii) lowering of the electron affinity, and (iii) the observation of a single peak at 1.27 eV corresponding to the  ${}^2E_{2u}$  benzene 1.5 eV resonance peak in electron transmission functions [19].

\*Corresponding author. Present address: Atomic and Molecular Physics Laboratories, RSPHySE, The Australian National University, Canberra ACT 0200, Australia. Email address: [cxm107@rsphysse.anu.edu.au](mailto:cxm107@rsphysse.anu.edu.au)

Currently, in some printing industries, toluene is widely employed as a cleaning solvent [21], but, once used, it is often simply released to the environment. Therefore efforts are being made to reduce the amounts of toluene used in a year and some proposals to remove toluene from the waste stream have been put forward [22]. Electron scattering data are fundamental for modeling these processes, which was one of the motivations for undertaking this project.

In this work we report on a joint study of electron impact TCSs, DCSs, elastic integral, and vibrational excitation cross sections for toluene molecules in an attempt to explore the origin of the resonances observed in the TCSs. We also report results for the TCSs for positron impact on toluene and compare the cross sections to those of the parent benzene molecule.

## II. PROCEDURES

### A. Total cross section (TCS) experiments

For these measurements a retarding potential time-of-flight (RP-TOF2) method was used. The apparatus has been reported in detail elsewhere [23] so is only briefly summarized here. The source for the electron and positron beams is a  $^{22}\text{Na}$  radioisotope with an activity of  $\sim 80 \mu\text{Ci}$ . The energy resolution, solely determined by the RPTOF experimental apparatus, is on average 0.3 eV at impact energies below 4 eV. However, the energy resolution is impact energy dependent and increases with increase in impact energy and is, for example, about 4 eV at 600 eV [24]. The TCS values were derived from the Beer-Lambert attenuation equation

$$Q_t = -\frac{1}{n\ell} \ln \frac{I_g}{I_v}; \quad (1)$$

where  $n$  is the number density of the target gas and  $I_g$  and  $I_v$  refer to the projectile beam intensities transmitted through the collision cell with and without the target gas, respectively.  $\ell$  refers to the effective length of the collision cell and was established by normalizing our measured positron- $\text{N}_2$  TCS to those of the positron- $\text{N}_2$  data of Hoffman *et al.* [25]. The energy calibration was done using positron- $\text{N}_2$  TOF spectra measured at 20 energies chosen at random in the range of 8–150 eV [26]. The toluene TCSs presented in this paper were confirmed to be pressure-independent in the present energy range by measurements of electron TCSs at the two fixed energies of 8 and 30 eV while varying the pressure in the range 0.4–10 mTorr. The maximum pressure used in the present measurements was 7.6 mTorr.

The TCS apparatus setup has specifically been designed to have a collision cell with wide entrance- and exit-apertures (3 mm in radius) because of the weak positron beam intensities. However, this brings with it the problem of forward scattered electrons-positrons being detected by the Ceratron detector, which is undesirable and thus needs to be corrected for. The procedure for this entails the use of DCS data for the molecule under study [27,28], which unfortunately is not available for either electron or positron impact with toluene, and thus the correction could not be carried out for the TCS data reported here. For benzene molecules, this

correction resulted in a TCS increase by a maximum 9% for electron impact and 12% for positron impact [14] but with no change in the TCS shape and energy dependence. It would be reasonable to expect similar corrections to apply for toluene.

The errors shown in the data in Table I are the summed uncertainties of contributions from counting statistics, gas pressure fluctuations, and the effective collision cell length calibration. They range from 5.4% to 6.4% for electron and 6.2%–11.3% for positron impact, respectively.

### B. Vibrational and elastic DCS experiments

These experiments were carried out using a crossed beam apparatus, which has already been described previously [29] so is only briefly summarized here. Incident electrons from a  $180^\circ$  monochromator intercept an effusive molecular beam at right angles and scattered electrons are energy analyzed in a second  $180^\circ$  hemispherical system. In order to maintain reasonably constant electron beam focusing and transmission at the interaction region, programmable power supplies are used to ramp the mid-element potentials of the monochromator exit and analyzer entrance lenses as required. Both the monochromator and the analyzer are enclosed in differentially pumped boxes to reduce the effect of the background gases and to minimize the stray electron background. The target molecular beam is produced by effusing the gas through a nozzle with an internal diameter of 0.3 mm and a length of 5 mm. The spectrometer and the nozzle are heated to a temperature of about  $70^\circ\text{C}$  to reduce the possibility of contamination during measurements. The overall energy resolution of the present measurements was about 35–40 meV, and the angular resolution was  $\pm 1.5^\circ$ .

The vibrational DCSs were measured while sweeping the impact energies from 1 to 30 eV for two loss energies of 0.17 and 0.38 eV, at a scattering angle of  $90^\circ$ . The elastic DCS presented was measured at 1.5 eV. Absolute cross sections for both measurements were obtained by the relative flow technique [30] using helium as the reference gas. Experimental errors in both vibrational excitation and elastic DCS are estimated to be of the order of 15%–20%.

### C. Elastic integral cross sections (ECSs): Theoretical method

The continuum multiple-scattering (CMS) method was used for computation of the elastic integral cross sections (ECSs) [31]. The CMS takes into account the many degrees of freedom of the electronic and nuclear motion and the non-spherical molecular fields in polyatomic molecules by employing some rather drastic techniques which makes numerical calculations tractable and less time-consuming, though with some reduction in accuracy. The scattering part of the method is based on the static-exchange-dipole potential model within the fixed-nuclei approximation. The configuration space is divided into three regions; the atomic, the interstitial, and the outer sphere surrounding the molecule, respectively. The Schrödinger equation in each region is solved numerically under separate boundary conditions, and by matching the wave functions and their derivatives from each region, the total wave functions of the scattered electron can

TABLE I. Toluene ( $C_6H_5CH_3$ ) electron and positron TCSs ( $\times 10^{-16} \text{ cm}^2$ ). Errors are as explained in the text.

Energy (eV)	Electron	Positron	Energy (eV)	Electron	Positron
0.2		37.8±4.3	11	65.7±3.6	45.0±2.8
0.4	32.4±2.1	41.8±4.3	12	64.8±3.5	45.6±2.9
0.6	32.8±2.0	51.1±4.7	13	63.0±3.5	42.6±2.7
0.8	35.5±2.1	53.6±4.8	14	60.1±3.3	41.7±2.8
1.0	38.1±2.1	54.7±3.7	15	58.5±3.3	41.6±2.8
1.2	40.6±2.3		16	57.7±3.3	40.6±2.9
1.3		56.2±3.8	17	57.5±3.3	41.1±2.9
1.4	41.2±2.3		18	54.9±3.2	39.9±2.9
1.6	40.0±2.2	57.7±4.0	19	53.9±3.1	40.2±2.9
1.8	39.2±2.2		20	52.7±3.2	39.9±2.9
1.9		57.7±4.0	22	51.5±3.1	38.9±2.6
2.0	38.6±2.2		25	49.1±2.7	38.6±2.7
2.2	37.7±2.1	57.9±3.9	30	48.0±2.7	37.1±2.4
2.5	38.2±2.2	55.4±3.8	35	46.4±2.6	
2.8	40.2±2.4	54.6±3.7	40	44.8±2.6	35.4±2.3
3.1	42.9±2.6	52.7±3.6	50	39.3±2.2	34.7±2.3
3.4	45.2±2.7	52.4±3.5	60	36.4±2.2	33.6±2.3
3.7	48.0±2.9	50.4±3.4	70	34.9±2.1	
4.0	53.3±2.9	50.5±3.2	80	32.2±2.0	31.5±2.2
4.5	55.5±3.0	48.2±3.1	90	30.0±1.8	
5.0	56.7±3.1	49.3±3.3	100	28.3±1.7	29.9±2.1
5.5	59.2±3.3	50.0±3.3	120	28.2±1.6	
6.0	61.5±3.4	49.2±3.2	150	26.0±1.5	25.1±1.9
6.5	66.3±3.7	48.2±3.3	200	22.3±1.2	22.9±1.7
7.0	67.4±3.8	49.0±3.2	250	20.8±1.2	21.3±1.6
7.5	69.1±3.8	47.6±3.2	300	17.9±1.0	17.4±1.3
8.0	68.8±3.8	47.4±3.3	400	16.0±1.0	15.9±1.4
8.5	70.8±3.8	48.6±3.4	500	13.8±0.9	14.1±1.1
9.0	68.1±3.7	48.4±3.3	600	11.8±0.8	12.1±1.0
9.5	67.1±3.7	47.8±3.3	800	8.9±0.7	9.3±0.8
10	66.3±3.6	47.3±3.0	1000	7.4±0.5	7.6±0.6

be determined and hence the scattering  $s$ -matrix. The scattering cross sections can be easily extracted from the  $s$ -matrix element by a standard procedure described earlier by Kimura and Sato [31].

### III. RESULTS AND DISCUSSION

Electron impact results are presented in Sec. III A and positron impact in Sec. III B. The electron and positron TCSs are compared in Sec. III C. The numerical values for the electron and positron TCSs are shown in Table I, together with the total uncertainties associated with each value.

#### A. Electron impact

##### 1. TCS

Figure 1(a) shows the current toluene ( $C_6H_5CH_3$ ) electron impact TCS results in comparison with those for the parent

benzene ( $C_6H_6$ ) molecules. The qualitative similarities between the TCSs for these two molecules include a decreasing TCS below 1.0 eV, the peak centered at 1.4 eV, the shoulder at 4.5 eV, the main peak at 8.0 eV, the shoulder at about 40 eV, and the monotonous decrease towards 1000 eV. The TCSs for these molecules are nearly equal to each other above 80 eV to within experimental error.

Electronically, in the ground state of  $C_6H_6$ , the configuration of the six valence electrons in the  $\pi$  orbitals shared by the carbon atoms is  $\bar{\chi}(a_{2u})^2(e_{1g})^4$  and the symmetry is  ${}^1A_{1g}$ . The ground state of the resonance temporarily forming  $C_6H_6^-$  is expected to have the configuration  $\bar{\chi}(a_{2u})^2(e_{1g})^4 {}^2E_{2u}$  [19]. The substitution of a benzene H atom by the  $CH_3$  radical alters the symmetry of the benzene ring, and the degenerate  $e_{2u}$  orbital of the benzene molecule is split into two. The attachment of the  $CH_3$  radical donates charge to the benzene ring and is expected to result in a splitting of the degenerate 1.5 eV  ${}^2E_{2u}$  resonance into two closely spaced peaks below and above 1.5 eV [19]. This phenomenon has been studied

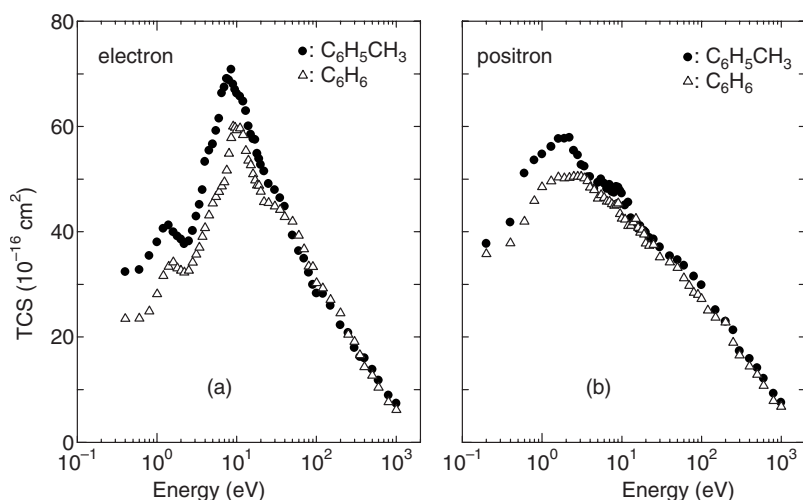


FIG. 1. Electron (a) and positron (b) TCSs for toluene ( $\text{C}_6\text{H}_5\text{CH}_3$ ) compared with results for benzene ( $\text{C}_6\text{H}_6$ ) from Ref. [14].

rather extensively in threshold-electron-excitation (TEE) spectra, and involves the trapping of slow projectile electrons temporarily by the molecule in its unoccupied  $\pi$  orbitals, resulting in short- and/or long-lived compound-negative-ion-resonant (CNIR) states. Early work by Christophorou *et al.* [7] reported a CNIR state at  $0.4 \pm 0.1$  eV. This is the lowest impact energy achieved in the present experiment but we see no indication of any structure at this energy. Electron transmission experiments have observed a second CNIR state at an energy of  $1.27 \pm 0.03$  eV [19]. An  $\text{SF}_6$  scavenger experimental technique also only observed a second CNIR state at an energy of  $1.45 \pm 0.3$  eV. Hence we assign the peak that we observe at  $1.4 \pm 0.3$  eV to the  $^2E_{2u}$  resonance.

The electron transmission experiments of Mathur and Hasted [19] also show resonance peaks at 3.1,  $4.9 \pm 0.1$ , and  $8.37 \pm 0.2$  eV. These authors identify the latter two peaks as two broad resonances corresponding to similar broad structures observed in benzene at around these energies. We do not observe the 3.1 eV peak feature reported by these authors. The reason for this is likely to be because the cross sections for these resonances are only about 1 to  $2 \text{ \AA}^2$ ; too small to be easily identified in the TCSs whose magnitudes are of the order of  $40 \text{ \AA}^2$  in this energy range. An unresolved shoulder is seen at about 4.5 eV in the benzene TCSs shown in Fig. 1(a). This can be attributed to the  $^2B_{2g}$  resonance in benzene observed by Cho *et al.* [13] at an energy of 4.94 eV. The 7–13 eV broad peak for benzene has been reported to be due to a  $^2E_{1u}$  shape resonance resulting from the temporary capture of an incident electron into the  $\sigma^*(e_{1u})$  orbital, as assigned by Allan [32]. The current toluene results show a broad shoulder centered at about 4.5 eV and the main broad peak at 8.0 eV, in good agreement with previous results to within experimental error. We thus associate them with these resonances.

The substitution of an H atom by the  $\text{CH}_3$  radical disturbs the symmetry of the benzene molecule so that toluene is weakly polar (0.375 D), compared to nonpolar benzene. This dipole moment in toluene is expected to result in a rising TCS at energies below about 1 eV, due to the dipole induced long range interaction. That this is not observed in the current results could either be that our lowest impact energy of 0.4 eV is still too high for this effect to be observable, or due

to the fact that it is overshadowed by the increasing number of rovibrational states that become available due to the addition of the functional group. Toluene TCS are larger than benzene TCS by, for example, 38% at the lowest energy of 0.4 eV, 23% and 22% at peak energies 1.5 and 8.5 eV, respectively. The different TCS magnitudes are only observed at energies below 100 eV, above this energy the TCS for the two molecules are almost equal within experimental error.

## 2. Probing the resonances in TCS: Vibrational and elastic DCS

In the elastic scattering channel, elastic scattering via resonances is in general masked by the direct elastic component. However, resonances can in most cases be clearly revealed in vibrational excitation functions for experiments done while sweeping impact energies across the resonance region. We employ this technique to probe the origin and nature of the resonances observed in the TCS. Figure 2 shows the toluene electron impact energy loss spectrum taken at a fixed impact energy of 7.5 eV and scattering angle of  $90^\circ$ .

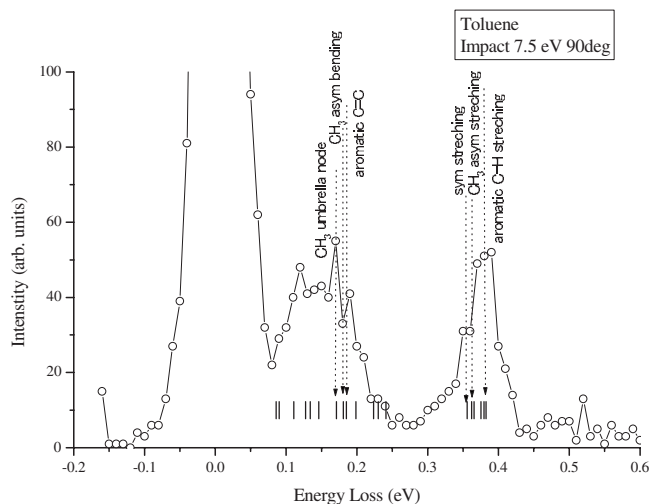


FIG. 2. Toluene electron impact energy loss spectrum. Vertical bars indicate the energies of the known vibrational mode frequencies [18].



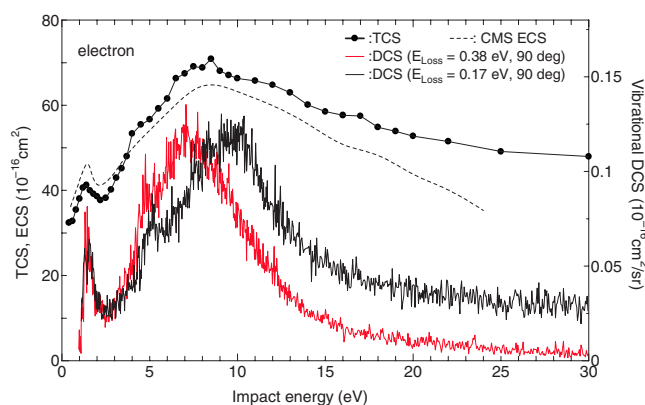


FIG. 3. (Color online) Toluene electron impact experimental TCS, vibrational excitation DCS, and the theoretical ECS. Note the different vertical scales for TCS and DCS.

Energy loss spectra were measured for two of the dominant fundamental modes of toluene, i.e., the  $\text{CH}_3$  asymmetric bend at energy loss of 0.17 eV, and the  $\text{CH}_3$  asymmetric stretch at energy loss of 0.38 eV. Figure 3 shows the experimental results of the vibrational functions for these modes over the impact energy range of 1 to 30 eV. Also shown in Fig. 3 are the TCS and theoretical elastic integral cross sections (CMS ECSs). Both the CMS ECS and the two sets of vibrational excitation DCSs show good qualitative reproduction of the structures observed in the TCSs. Below 4 eV, however, the CMS ECS clearly overestimates the cross sections, as they become greater than the TCS.

Both the CMS ECS and the two sets of vibrational excitation DCSs show the 1.4 eV resonance peak, in agreement with the TCS results. Despite the overestimation of the cross sections by the CMS ECS at the 1.4 eV resonance, it is clear that the elastic scattering channel dominates the scattering events below 5 eV. Note that the TCS and CMS ECS have units of  $10^{-16} \text{ cm}^2$  while the vibrational excitation DCSs have units of  $10^{-18} \text{ cm}^2/\text{sr}$ . Nevertheless, it is also clear that both the  $\text{CH}_3$  asymmetric bending and  $\text{CH}_3$  asymmetric stretching vibrational modes nearly equally contribute to the 1.4 eV resonance. Similar results are observed for the resonance feature at about 4.5 eV, albeit with the stretching mode being stronger than the bending mode. The current results show that the broad main resonance spanning the energy range 7–13 eV is actually made up of two resonance peaks, vibrational in origin, centered at about 7 eV ( $\text{CH}_3$  asymmetric stretching) and at 9.3 eV ( $\text{CH}_3$  asymmetric bending), with nearly equal magnitudes at their respective peak energies. It is also important to point out that there could be other vibrational states making contributions to the TCS as well at these resonance energies. Both the ECS and the two sets of vibrational cross sections decrease gradually beyond 12 eV. This decrease is expected to be associated with corresponding increases in the importance of the ionization and electronic excitation channels.

We took further interest in investigating the nature of the 1.4 eV peak commonly observed in both vibrational modes and attributed to the second CNIR state of the  ${}^2E_{2u}$  resonance in the TCS. With a fixed impact energy of 1.5 eV, elastic DCSs were measured over the angular range  $15^\circ$ – $130^\circ$ .

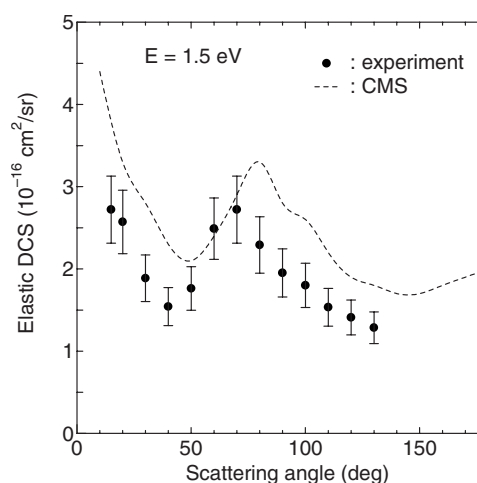


FIG. 4. Electron impact experimental and theoretical elastic DCSs for toluene at an impact energy of 1.5 eV.

CMS calculations were also performed over the angular range  $10^\circ$ – $180^\circ$ . The results are shown in Fig. 4.

Both the experimental and theoretical results show a similar general trend for the angular dependence of the cross sections in the region of the resonance with a rising DCS towards the forward scattering angle of  $0^\circ$ , a peak at  $50^\circ$ – $100^\circ$  and a decreasing DCS beyond  $100^\circ$ . Overall the CMS results are shifted by about  $10^\circ$  to higher angles.

## B. Positron impact

Figure 1(b) shows the toluene positron TCS in comparison with similar data for the parent benzene molecule. There is a qualitative similarity between the two TCSs including a broad peak commonly centered at about 1.5 eV, unclear features in the region of 4–9 eV, and a shoulder centered at about 50 eV. As in the electron impact case, the positron TCS does not show an increase in magnitude at the lowest impact energies within the present range of measurement ( $E_i > 0.2 \text{ eV}$ ) as would be expected for polar molecules due to the dipole induced long-range interaction. The significant enhancement of the cross sections towards the peak at 1.5 eV could be due to the substitution of the H atom in benzene by the  $\text{CH}_3$  radical in toluene, possibly resulting in an increased cross section for rovibrational scattering. The non-negligible features in the region 4–9 eV may be attributed to electronic excitation, although positronium formation, with a threshold energy ( $E_{Ps}$ ) of 2.02 eV may not be excluded. Generally toluene TCSs are greater than those for benzene at energies below 100 eV. Above this energy, the positron and electron impact TCSs are very similar in magnitude.

## C. Electron and positron TCSs compared

Figure 5 compares the toluene electron and positron TCSs. Some features worth highlighting from these results are as follows: (i) the positron TCSs are up to 30% greater than electron TCSs below 3.5 eV, and (ii) both spectra exhibit low energy peaks at about 1.4 eV.

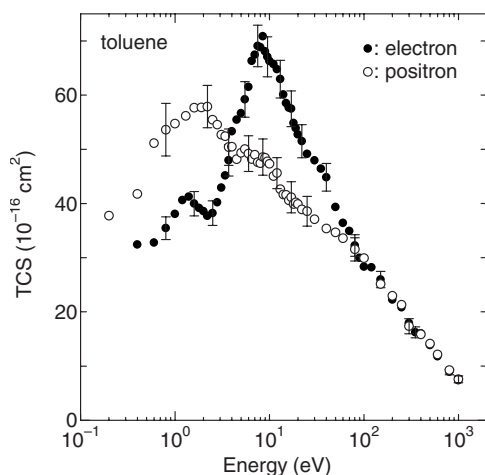


FIG. 5. Electron and positron TCSs for toluene molecules.

As discussed above for electron impact excitation, the larger contribution to the cross sections up to 1.5 eV may be due to the increasing number of rovibrational states that become available due to the presence of the  $\text{CH}_3$  radical. As for the greater magnitude of the positron TCS, this could be an indication of enhancement of the rovibrational excitation by a (temporary) bound positron state. The magnitude difference between these TCSs is such that, for example, positron TCSs are greater than their electron counterpart by 29% at 1.4 eV, while electron TCSs are greater than positron TCSs by about 46% at 8.5 eV. The larger electron TCS in the 4–18 eV region is due to several resonances contributing to the observed spectrum. Above 100 eV, the electron and positron TCSs nearly merge with each other; a behavior that is

expected in an impact energy range where the first Born approximation is valid.

#### IV. CONCLUSION

In this paper, the first electron and positron scattering cross sections from toluene are reported. Peaks were observed in the electron TCS at 1.4, 4.5, 8.0, and 40 eV. The first three peaks were also observed in vibrational excitation spectra and attributed to the  ${}^2E_{2u}$  compound-negative-ion-resonance and the  ${}^2B_{2g}$  and  ${}^2E_{1u}$  shape resonances, respectively, inferred from a comparison with benzene. Elastic DCS studies showed the 1.5 eV peak to be resonant in nature. The current vibrational excitation DCS results further showed that the broad peak centered at 8 eV probably consists of many overlapping peaks; with the results for the  $\text{CH}_3$  asymmetric stretch at 7 eV and the asymmetric bend at 9.3 eV. Positron TCS showed a peak at about 1.4 eV, unclear features in the region for 4–9 eV, and a shoulder centered at about 50 eV. The effect of  $\text{CH}_3$  substitution for the H atom in benzene showed up as a larger TCS compared to benzene for both electron and positron impact below 100 eV. Toluene positron TCSs are conspicuously larger than their electron counterpart below 4 eV, electron TCSs are greater than positron TCSs at energies 4–100 eV.

#### ACKNOWLEDGMENTS

The work was supported in part by a Grant-in-Aid from the Ministry of Education, Science, Technology, Sport and Culture, Japan, the Japan Society for the Promotion of Science (JSPS); and a Cooperative Research Grant from the National Institute for Fusion Science (NIFS). C.M. is also grateful to Yamaguchi University as he did part of this work while he was a Ph.D. student there.

- 
- [1] M. Matsuzawa, *J. Phys. Soc. Jpn.* **18**, 1273 (1963).  
 [2] F. H. Read and G. L. Whiterod, *Proc. Phys. Soc. Jpn.* **85**, 71 (1965).  
 [3] W. E. Wentworth, L. W. Kao, and R. S. Becker, *J. Phys. Chem.* **79**, 1161 (1975).  
 [4] L. G. Christophorou, R. P. Blaunstein, and D. Pittman, *Chem. Phys. Lett.* **22**, 41 (1973).  
 [5] H. Shimamori, Y. Tatsumi, and T. Sunagawa, *J. Chem. Phys.* **99**, 7787 (1993).  
 [6] J-F. Gal, S. Geribaldi, G. Pfister-Guillouzo, and D. G. Morris, *J. Chem. Soc., Perkin Trans. 2* **2**, 103 (1985).  
 [7] L. G. Christophorou, D. L. McCorkle, and J. G. Carter, *J. Chem. Phys.* **60**, 3779 (1974).  
 [8] S. L. Lunt, D. Field, S. V. Hoffmann, R. J. Gulley, and J-P. Ziesel, *J. Phys. B* **32**, 2707 (1999).  
 [9] J. K. Olthoff, J. A. Tossell, and J. H. Moore, *J. Chem. Phys.* **83**, 5627 (1985).  
 [10] L. Sunche and G. J. Schulz, *J. Chem. Phys.* **58**, 479 (1973).  
 [11] W. Holst and J. Holtsmark, *K. Norsk. Vidensk. Selsk.* **4**, 89 (1931).  
 [12] R. Azaria and G. J. Schulz, *J. Chem. Phys.* **62**, 573 (1975).  
 [13] H. Cho, R. J. Gulley, K. Sunohara, M. Kitajima, L. J. Uhlmann, H. Tanaka, and S. J. Buckman, *J. Phys. B* **34**, 1019 (2001).  
 [14] C. Makochekanwa, O. Sueoka, and M. Kimura, *Phys. Rev. A* **68**, 032707 (2003).  
 [15] D. E. Teets and D. H. Andrews, *J. Chem. Phys.* **3**, 175 (1935).  
 [16] P. M. Chu, F. R. Guenther, G. C. Rhoderick, and W. J. Lafferty, *J. Res. Natl. Inst. Stand. Technol.* **104**, 59 (1999).  
 [17] J. Ree, K. S. Chang, Y. H. Kim, and H. K. Shin, *Bull. Korean Chem. Soc.* **24**, 1223 (2003).  
 [18] M. Boruta, M. Hachey, A. Bogomolov, E. Karpushkin, and T. Williams, see their homepage at [www.acdlabs.com](http://www.acdlabs.com)  
 [19] D. Marthur and J. B. Hasted, *J. Phys. B* **9**, L31 (1975).  
 [20] R. N. Compton, R. H. Huebner, P. W. Reinhardt, and L. G. Christophorou, *J. Chem. Phys.* **48**, 901 (1968).  
 [21] See <http://www.pneac.org/sheets/all/Biochemicals-for-the-Printing-Industry.pdf>  
 [22] See <http://www.fujitsu-ten.co.jp/english/ecology/2004/2004report12-14e.pdf>  
 [23] O. Sueoka, S. Mori, and A. Hamada, *J. Phys. B* **27**, 1452 (1994).  
 [24] M. Kimura, C. Makochekanwa, and O. Sueoka, *J. Phys. B* **37**, 1461 (2004).

- [25] K. R. Hoffman, M. S. Dababneh, Y. F. Hsieh, W. E. Kauppila, V. Pol, J. H. Smart, and T. S. Stein, *Phys. Rev. A* **25**, 1393 (1982).
- [26] O. Sueoka and S. Mori, *J. Phys. B* **19**, 4035 (1986).
- [27] A. Hamada and O. Sueoka, *J. Phys. B* **27**, 5055 (1994).
- [28] O. Sueoka, C. Makochekanwa, and H. Kawate, *Nucl. Instrum. Methods Phys. Res. B* **192**, 206 (2002).
- [29] H. Tanaka, T. Ishikawa, T. Masai, T. Sagara, L. Boesten, M. Takekawa, Y. Itikawa, and M. Kimura, *Phys. Rev. A* **57**, 1798 (1998).
- [30] S. K. Srivastava, A. Chutjian, and S. Trajmar, *J. Chem. Phys.* **63**, 2659 (1975).
- [31] M. Kimura and H. Sato, *Comments At. Mol. Phys.* **26**, 333 (1991).
- [32] M. Allan, *J. Electron Spectrosc. Relat. Phenom.* **48**, 219 (1989).